Theoretical analysis of coupled effects of microbe and root architecture on methane oxidation in vegetated landfill covers

Feng, S.; Leung, A. K.; Ng, C. W. W.; Liu, H. W.

Published in:
Science of the Total Environment

DOI:
10.1016/j.scitotenv.2017.04.025

Publication date:
2017

Theoretical analysis of coupled effects of microbe and root architecture on methane oxidation in vegetated landfill covers

S. Feng, A.K. Leung, C. W. W. Ng and H.W. Liu*

Name: Dr Song Feng
Title: Postdoctoral fellow
Affiliation: Department of Civil and Environmental Engineering, Hong Kong University of Science and Technology

---

Name: Dr Anthony Kwan Leung
Title: Senior lecturer in Civil Engineering
Affiliation: School of Science and Engineering, University of Dundee

---

Name: Dr Charles Wang Wai Ng
Title: Chair Professor of Civil and Environmental Engineering
Affiliation: Department of Civil and Environmental Engineering, Hong Kong University of Science and Technology

---

Name: Ms Hong Wei Liu* (Corresponding author)
Title: Doctoral research student
Affiliation: Department of Civil and Environmental Engineering, Hong Kong University of Science and Technology
Address: Department of Civil and Environmental Engineering, Hong Kong University of Science and Technology, Clear Water Bay, Kowloon, Hong Kong
E-mail: hliuan@connect.ust.hk
Tel: +852 6849 4779

Abstract

Reduction of soil moisture by plant root-water uptake could improve soil aeration for microbial aerobic methane oxidation (MAMO) in a landfill cover, but excessive soil moisture removal could suppress microbial activity due to water shortage. Existing models ignore the coupled microbe-vegetation interaction. It is thus not known whether the presence of plants is beneficial or adverse to MAMO. This study proposes a newly-improved theoretical model that couples the effects of root-water uptake and microbial activity for capturing water-gas flow and MAMO in unsaturated soils. Parametric studies are conducted to investigate the effects of root characteristics and transpiration rate on MAMO efficiency. Uniform, parabolic, exponential and triangular root architectures are considered. Ignoring the effects of water shortage on microbe over-predicts the MAMO efficiency significantly, especially for plants with traits that give high root-water uptake ability (i.e., uniformly-rooted and long root length). The effects of plants on MAMO efficiency depends on the initial soil moisture strongly. If the soil is too dry (i.e., close to the permanent wilting point), plant-water uptake, with any root architecture considered, would reduce MAMO efficiency as further soil water removal by plants suppresses microbial activity. Plants with exponential or triangular root architectures could preserve 10% higher MAMO than the other two cases. These two architectures are more capable of minimizing the adverse effects of root-water uptake due to microbial water shortage. This implies that high-water-demand plants such as those with long root length and with uniform or parabolic root architectures require more frequent irrigation to prevent from excessive reduction of MAMO efficiency.

Key words: plant root-water uptake; microbial aerobic methane oxidation; coupled water-gas flow; numerical simulation

1 Introduction

Effects of vegetation on microbial aerobic methane oxidation (MAMO) in landfills have drawn significant attention by environmentalists and engineers, who are responsible for the mitigation of methane gas emission. It is well known that the amount of soil water content affects MAMO significantly (Czepiel et al., 1996; Spokas and Bogner, 2011; Abichou et al., 2011; Scheutz et al., 2009; Zhang et al., 2012). The presence of plants could be beneficial to MAMO. Through root-water uptake, reduction of soil moisture would increase gas permeability and diffusion, improving soil aeration (i.e., more oxygen is available) (Bohn et al, 2011; Reichenauer et al., 2011; Hilger et al., 2000; Zhang et al., 2013). However, plant transpiration, on the other hand, could be adverse to MAMO (Tanthachoon et al., 2008). When soil water content is reduced below the soil field capacity (Abichou et al., 2011), the activity of methanotrophic bacteria in soil would be inhibited, suppressing MAMO. It is clear that vegetation plays an important role on the performance of landfills in terms of the control of landfill gas emission. More detailed investigation on the coupled soil-plant-water-gas interaction is needed.

Plants can develop different root architectures at specific environmental conditions, such as, uniform, triangular, exponential and parabolic shapes (Fig.1). Experiments (Kamchoom et al., 2014; Ng et al., 2016; Leung et al., 2016) and analytical modelling (Prasad, 1988; Ng et al., 2015a) all shows that transpiration induced by different root architectures could result in significantly different magnitudes and distributions of pore-water pressure and soil water content. A few experimental studies (Bohn et al, 2011; Reichenauer et al., 2011; Hilger et al., 2000; Wang et al., 2008) have attempted to investigate the vegetation effects on MAMO. However, effects of different root architectures on MAMO and its efficiency are not known. It is crucial for

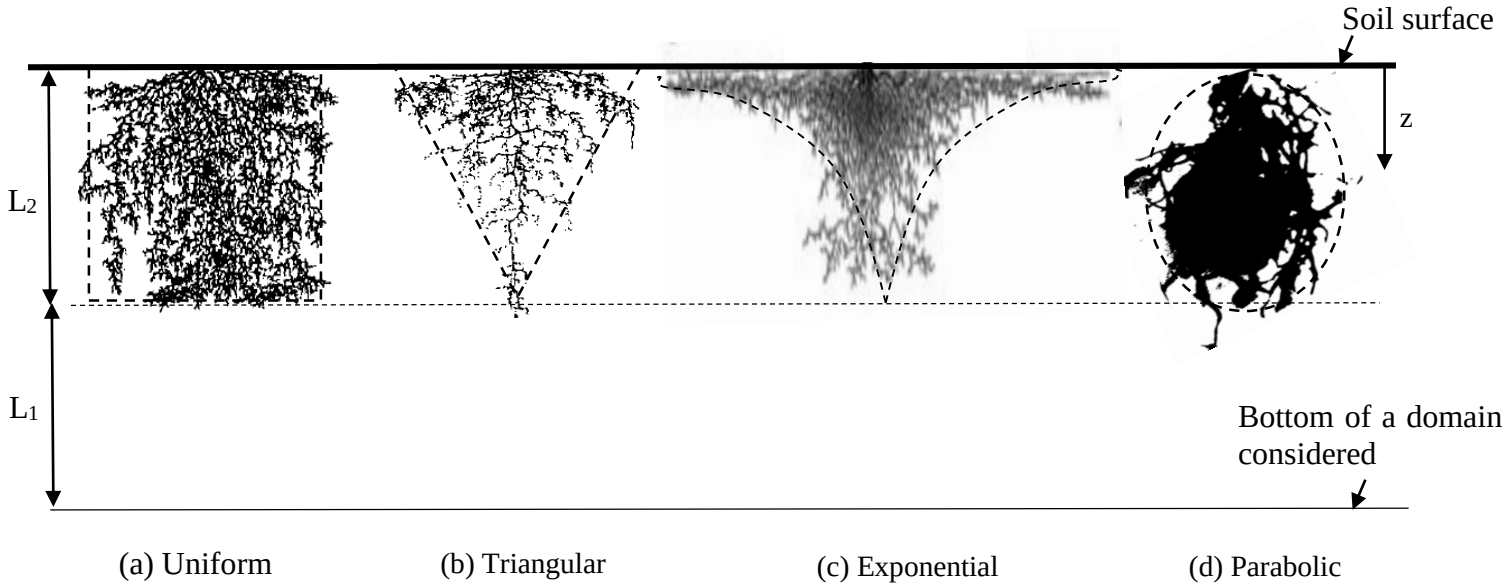

Figure 1 The four different idealized root architectures considered in this study (after Ng et al., 2015a)

landfill/ecological engineers to select appropriate plant species which have favorable root architectures that could enhance the performance of the landfill cover.

In fact, experimental study on the effects of root architectures on MAMO could be challenging. It is because plants have multiple effects on soil responses which are often coupled and difficult to be isolated from each other. For example, root-water uptake due to different combinations of root architectures and root depths would induce different magnitude and distribution of soil water content (Ng et al., 2015a; Prasad, 1988). Numerical modelling, on the contrary, is a useful means that can systematically investigate the relative importance and significance of each individual factor on MAMO. Although there have been various numerical models that could capture MAMO (De Visscher and Cleemput, 2003; Molins et al., 2008; Stein et al., 2001; Ng et al., 2015b), the effects of plant root-water uptake are generally ignored. Abichou et al. (2015) developed a theoretical model to attempt to investigate the effects of vegetation on MAMO, yet, the influence of root architectures on MAMO are not considered. Moreover, the effects of soil water content on the activity of methanotrophic bacteria involved in MAMO are also ignored in their model. Hence, their model is not able to capture the adverse effects of water shortage on microbial activity due to extensive root water-uptake during MAMO.

The objective of this study is thus to use numerical modelling technique to provide new insights into the coupled effects of plant root-water uptake on microbial activities on MAMO efficiency considering different root architectures. Effects of plant root-water uptake on MAMO are newly introduced into the previous theoretical model proposed by Ng et al. (2015b). The newly improved model could consider coupled microbe-plant interaction during water-gas flow in

unsaturated soils. The root-water uptake modelling also enables the effects of four different root architectures, namely uniform, parabolic, exponential and triangular, to be considered when assessing MAMO efficiency. A series of parametric studies were then carried out to identify critical factors of plants that affect MAMO efficiency, including root architectures (triangular, parabolic, exponential and uniform), transpiration rate and root depth.

2 Theoretical model and numerical methods

2.1 Theoretical model

The newly revised theoretical model reported in this study is based on the formulation proposed by Ng et al. (2015b). Based on the principle of mass conservation, the governing equations for water and multicomponent gas reactive transfer were derived. The model had been validated by Ng et al. (2015b), Feng et al. (2017) and Feng (2016) for coupled water-gas-heat reactive transfer with MAMO, against the experimental data reported by De Visscher et al. (1999) and Berger et al. (2005), respectively.

In this study, the governing equation for water transfer is newly-modified by considering plant root-water uptake via a sink term, as follows:

$$\frac{\partial}{\partial t}[\rho_w \theta_w] = -\nabla(\rho_w v_w) + \rho_{DB} M_{H_2O} r_w - \rho_w S(\psi, z)\mathrm{H(z)} \quad (1)$$

where t is time; ρ_w is water density; θ_w is volumetric water content (VWC); v_w is velocity of Darcian water flow; ρ_{DB} is dry bulk density of soil; M_{H_2O} is molar mass for water; r_w is water generation rate by per unit mass of dry soil; $S(\psi, z)$ is sink term associated with plant root-water

uptake as a function of matric suction ψ (defined as the difference between gas pressure P_g and pore-water pressure P_w) and depth *z*. The sink term is defined as the volume of water transpired by a plant per unit volume of soil and per unit time (Feddes et al., 1976). H(z) is the Heaviside function (Polyanin, 2002) defined as

$$\mathrm{H}(z)=\begin{cases}1 & 0\le z\le L_2 \quad \text{Within root zone}\\ 0 & L_2\le z\le (L_1+L_2) \quad \text{Outside root zone}\end{cases} \tag{2}$$

where L_2 is the root depth; and L_1 is the length outside the root zone, as defined in Fig.1.

The term on the left hand side of Eq. (1) represents the net changes in liquid water per unit volume of soil, as a result of the processes described on the right hand side of the equation, including the transfer of liquid water (the first term), water generated by MAMO (the second term) and root-water uptake (the third term).

In unsaturated soil, the velocity of Darcian water flow (v_w in Eq. (1)) is described as follow:

$$v_w=-k_w\left(\nabla\frac{P_w}{\rho_w g}+1\right) \tag{3}$$

where k_w is water permeability function; ρ_w is the specific weight of water; and *g* is gravitational acceleration. Any plant-induced changes in infiltration rate or water permeability k_w (Beven and Germann, 1982) were not taken into account.

144 The use of sink term ($S(\psi,z)$) to capture the process of plant root-water uptake has been
145 verified and frequently used in theoretical models to investigate subsurface water flow for
146 various engineering problems (Feddes et al., 1978; Ng et al., 2015a; Nyambayo and Potts, 2010).
147 Based on Feddes et al. (1976), root-water uptake ($S(\psi,z)$) can be described as:

148 $$S(\psi,z)=\alpha(\psi)G(z)T_p \tag{4}$$

149 where T_p is transpiration rate and $\alpha(\psi)$ is the so-called transpiration reduction function that
150 varies with ψ as follows:

151 $$\alpha(\psi)=\begin{cases} 0 & \psi \le \psi_{os} \\ 1 & \psi_{os} < \psi \le \psi_{ws} \\ \dfrac{\psi_{wilt}-\psi}{\psi_{wilt}-\psi_{ws}} & \psi_{ws} < \psi \le \psi_{wilt} \\ 0 & \psi > \psi_{wilt} \end{cases} \tag{5}$$

152 where ψ_{os} (anaerobiosis point) is the suction corresponding to oxygen stress, when root-water
153 uptake is negligible due to lack of aeration caused by high soil water content; ψ_{ws} (turning point)
154 refers to the suction related to water stress, when roots have reduced ability to extract water from
155 soil to prevent excessive plant water loss; and ψ_{wilt} is the suction at permanent wilting point,
156 when root can no longer extract water from soil due to too low soil water content.
157
158 According to Eq. (5), root-water uptake would occur when suction is higher than ψ_{os} as oxygen
159 stress relieves but lower than ψ_{ws} before plant wilts. The ability of root-water uptake is
160 maximum between ψ_{os} and ψ_{ws}, beyond which the ability decreases linearly with suction to

161 ψ_{wilt} . $G(z)$ in Eq. (4) describes the distributions of root-water uptake ability, which in this study

162 is assumed to be proportional to root architecture with depth z. Four idealized root architectures

163 can thus be mathematically expressed as:

164
$$G(z)=\begin{cases}\dfrac{1}{L_2} & \text{Uniform root architecture}\\ \dfrac{2}{L_2}\left(\dfrac{L_2-z}{L_2}\right) & \text{Triangular root architecture}\\ \left[\dfrac{\beta\exp(\beta L_2-\beta z)-\beta}{\exp(\beta L_2)-\beta L_2-1}\right] & \text{Exponential root architecture}\\ \dfrac{2}{L_2}\left[\dfrac{3((L_2-z)L_2-(L_2-z)^2)}{{L_2}^2}\right] & \text{Parabolic root architecture}\end{cases} \quad (6)$$

165 In Eq. (6), β is a constant with a unit of m^{-1}, which controls the curvature of exponential root

166 architecture. A case study reported by Raats (1974) suggests that β is equal to 1 m^{-1}. The total

167 root area for each root architecture is considered to be the same for fair comparison. The

168 distributions of transpiration-induced suction by these four root architectures have been verified

169 by Ng et al. (2015a).

170

171 In order to quantify the water generation by MAMO (i.e., r_w in Eq. (1)), the following

172 stoichiometry suggested by De Visscher and Cleemput (2003) may be used:

173
$$CH_4+1.5O_2\rightarrow 0.5CO_2+1.5H_2O+0.5-CH_2O- \quad (7)$$

where $-CH_2O-$ represents biomass. The rate of MAMO may be described by the dual-substrate Michaelis–Menten kinetics, taking into account the effects of temperature and soil water content on oxidation rate (Abichou et al., 2011), as follows:

$$r_g^{CH_4} = -f_{V,T} f_{V,m} \frac{V_{\max} y_{CH_4}}{K_m + y_{CH_4}} \cdot \frac{y_{O_2}}{K_{O_2} + y_{O_2}} \quad (8)$$

where V_{max} denotes the maximum methane oxidation rate per unit mass of dry soil; K_m and Ko_2 represent half saturation constants for methane and oxygen, respectively; $f_{V,T}$ and $f_{V,m}$ describe effects of temperature and water content on microbial activity, respectively. Details for $f_{V,T}$ and $f_{V,m}$ can be found in the Part 1 of the supplementary information (SI); y_{CH_4} and y_{O_2} denote volume fraction of methane and oxygen, respectively. Based on ideal gas law, volume fraction of gas k equals to its mole fraction (i.e., $y_k = \frac{c_g^k}{\sum_{j=1}^{4} c_g^j}$). Through Eq. (8), the effects of root-water uptake on the improvement of soil aeration (i.e., $f_{O_2} = \frac{y_{O_2}}{K_{O_2} + y_{O_2}}$ increases) and the suppression of microbial activity of MAMO due to shortage of water (i.e., $f_{V,m}$ decreases) can be modelled. In order to reveal the dominant mechanism for these two counteracting mechanisms, the following dimensionless ratio is defined:

$$\eta = \frac{f_{O_2}}{f_{V,m}} = \frac{\left(\frac{y_{O_2}}{K_{O_2} + y_{O_2}} \right)}{f_{V,m}} \quad (9)$$

When η is larger than 1, the MAMO is more predominantly affected by the water shortage on microbial activity. In contrast, when it is smaller than 1, the lack of soil aeration (hence oxygen

transfer) is the more dominant mechanism that reduces MAMO. When $\eta > 1$, the following dimensionless ratio, namely water shortage coefficient, is defined to estimate the extent to which water availability affects MAMO:

$$\varpi = \frac{T_p * t}{(\theta_{ini} - \theta_{wilt})L_2} \quad (10)$$

where θ_{ini} and θ_{wilt} refer to initial VWC and VWC at permanent wilting point (ψ_{wilt}), respectively. The numerator ($T_p * t$) represents the maximum root-water uptake (i.e., $\alpha(\psi)$ = 1; Eq. (5)) for a period of *t*; The denominator represents the minimum amount of soil water available for root-water uptake, ignoring any water supply from outside a root zone. When ϖ ? 1, the soil water content would not meet the demand of root-water uptake, and it is the opposite when $\varpi \le 1$. A higher ϖ means an increased effects of water shortage on MAMO.

In order to further evaluate any improvement provided by vegetation, MAMO efficiency is defined as follows (De Visscher et al., 1999):

$$\eta_{oxi} = \frac{\Gamma_{CH_4}^{in} - \Gamma_{CH_4}^{out}}{\Gamma_{CH_4}^{in}} \times 100\% \quad (11)$$

where $\Gamma_{CH_4}^{in}$ and $\Gamma_{CH_4}^{out}$ are the methane influx and outflux, respectively; and η_{oxi} is the MAMO efficiency. The theoretical consideration for MAMO and governing equation for each gas component transfer (Eq. (A3) in Part 2 of the SI) are identical to that presented in Ng et al. (2015b). The governing equations for gas transfer were derived based on the principle of mass conservation. The gas species considered in this study includes CH_4, carbon dioxide (CO_2), oxygen (O_2) and nitrogen (N_2). Gas transfer mechanisms considered include gas dissolution in liquid water, gas advection and molecular diffusion and gas reaction involved in MAMO.

2.2 Numerical implementation and parameterization

In this study, one-dimensional (1D) numerical simulation was conducted, following the identical boundary conditions and procedures used in the soil column test performed by De Visscher et al. (1999) for bare soil. In their column tests, sandy loam (following the classification method by USDA 1998) was used. The test was conducted at an ambient temperature of 22 °C. In their test, a plexiglass cylinder with height of 0.5 m and inner diameter of 0.141 m was used. The height of soil column tested is 0.5 m. At the column bottom, methane and carbon dioxide were applied at a constant flux of 13.4 mol m^{-2}_{column} d^{-1}. The head space of the column was continuously flushed by humidified air through water-washing bottle. This procedure aimed to mitigate the effects evaporation on MAMO efficiency. Indeed, their measurements showed that the variations of soil water content was less than 2% after testing for about 56 days. Hence, any effects of evaporation can be neglected.

After validating the theoretical model against the published data of the bare soil column tests by Ng et al. (2015b), this study adds the vegetation effects for parametric study. Note that because the lateral wall of the soil column adopted by De Visscher et al. (1999) was thermally conductive, any effect of heat generated by MAMO on soil temperature was found to be negligible (Ng et al. 2015b). Thus, heat transfer can be ignored in this study. It should also be noted that although there are some laboratory tests that investigated the effects of vegetation on MAMO (Bohn et al, 2011; Reichenauer et al., 2011; Hilger et al., 2000; Wang et al., 2008), it is unfortunate that these studies could not be used for model validation in this study because the root architectures considered in each of these studies were not known or reported.

The finite element software, COMSOL, was used for numerical implementation and simulation. According to the test conditions presented by De Visscher et al. (1999), the 1D numerical model with a height of 0.5 m was built. Four root architectures with different L_1 and L_2 were specified in the top part of the soil column. The root depth, L_2, ranged from 0.1 to 0.5 m was considered in this study. The input material properties are summarized in Table 1. The soil properties and kinetics parameters for MAMO were measured by De Visscher et al. (1999). These parameters had been adopted for the calibration of the theoretical model for coupled water-gas-heat reactive transfer with MAMO by Ng et al. (2015b) using the same bare soil column reported by De Visscher et al. (1999). The parameters of soil hydraulic properties, Henry's constant and binary diffusion coefficients for each gas component transfer were determined based on the calibrated parameters reported by Ng et al. (2015b). As a first approximation to describe the transpiration reduction function in Eq. (5), typical values of 40 and 1500 kPa were taken for ψ_{ws} and ψ_{wilt} (Feddes et al., 1976), respectively, for all four root architectures.

A constant transpiration rate was specified over the entire root zone, considering a range of 1 to 6.6 mm/day (Leung and Ng (2013)) in this parametric study. A zero-water-flux boundary was specified at the column surface. This aims to simulate no-evaporation condition, consistent with the test conditions reported by De Visscher et al. (1999).

Table 1 Summary of input parameters for the numerical simulation

Parameter		Value	Source
Porosity		0.587	De Visscher et al., 1999
Soil dry bulk density ($kg\ m^{-3}$)		1039	
Soil particle density ($kg\ m^{-3}$)		2521	
Hydraulic parameters[a]	Saturated volumetric water content, $\theta_{saturated}$	0.587	Ng et al. (2015b)
	Residual volumetric water content, θ_r	0.02	
	Van Genuchten's parameter, m	0.33	
	Van Genuchten's parameter, a (m^{-1})	5	
	Intrinsic permeability k_i (m^2)	$5.8*10^{-12}$	
	Water density (kg/m^3)	1000	
Henry's constant (dimensionless)	CO_2	0.8145	
	O_2	0.0318	
	N_2	0.0159	
	CH_4	0.0316	
Binary diffusion coefficient ($10^{-6}\ m^2s^{-1}$)	O_2 and N_2	2.083	
	CO_2 and N_2	1.649	
	CH_4 and N_2	2.137	
	CO_2 and O_2	1.635	
	O_2 and CH_4	2.263	
	CO_2 and CH_4	1.705	
Kinetics parameters for MAMO	Maximum methane oxidation rate (mol $kg^{-1}\ s^{-1}$)[b]	$7.5*10^{-7}$	De Visscher et al., 1999
	K_{o2}	0.012	
	K_{ch4}	0.0066	
Root water uptake	Anaerobiosis point ψ_{os} (kPa)	1	Feddes et al. (1976)
	Turning point ψ_{ws} (kPa)	40	
	Wilting point ψ_{wilt} (kPa)	1600	

Note:

(a) Soil water characteristic curve is based on expression proposed by Van Genuchten (1980), while water permeability function is based on Mualem (1976).

(b) Based on De Visscher et al. (2003), for the top 0.2m depth, a constant maximum methane oxidation rate of $7.5*10^{-7}$ mol $kg^{-1}_{dry\ soil}\ s^{-1}$ is adopted; for 0.2 m to 0.5 m depths, maximum methane oxidation rate is considered to decrease linearly from $7.5*10^{-7}$ mol $kg^{-1}_{dry\ soil}\ s^{-1}$ to zero.

On the other hand, constant gas molar concentration boundary was also specified at the column surface for each gas component, according to the concentration of each gas in the atmosphere (De Visscher and Cleemput, 2003). The bottom boundary was a unit-gradient flux condition (i.e., gravity-induced flux) for water transfer. For the gas transport, a zero flux condition was applied for nitrogen (N_2) and oxygen (O_2), while a constant influx of 13.4 mol m^{-2}_{column} d^{-1} for methane (CH_4) and carbon dioxide (CO_2).

Two initial uniform distributions of soil VWC were considered, 17.2% (referred to as "dry" condition; the initial value considered by De Visscher et al. (1999)) and 36.8% (referred to as "wet" condition"). These two initial VWCs correspond to ψ_{ws} and ψ_{os}, respectively, according to the soil water retention curve inputted (see Table 1). The initial concentration for each gas component in the soil was considered to be the same as that in the atmosphere. Subsequently, transient analysis was commenced by simulating a continuous supply of the constant fluxes of CH_4 and CO_2 for 34 days at the bottom of the soil column, while allowing the plant near the column surface to transpire under a constant rate. The duration of 34 days is the maximum no-rainfall period between 2004 and 2014 recorded by Hong Kong Observatory (2015). This represents a kind of "worst-case" scenario because it might be less common for any climate region to have prolonged drying period of 34 days.

2.3 Analysis scheme for parametric study

In total, three series of 1D transient analyses of the 0.5 m vertical soil column, with and without vegetation, were carried out. These analyses aim to provide insights into the role of vegetation on the performance of the flat ground part of a landfill cover, where water and gas transfer is likely

to be 1D. The objective of the first series of analysis is to highlight the importance to consider the coupled effects of microbes and plant root-water uptake on MAMO using the model newly-improved in this study. The second and third series of analyses consider the coupled microbes-vegetation interaction for investigating the effects of the four root architectures (Fig. 1) and the amount of transpiration rate (Eq. (4)) on MAMO efficiency, respectively. In the second and third series, the effects of the initial wetness of the soil column (i.e., different initial VWCs) were also studied, as it has a direct influence on the ability of plant root-water uptake (Eq. (5)) and hence MAMO efficiency (Eq. (11)). The analysis plan is summarized in Table 2.

3 Results and discussion

3.1 Importance of coupled microbe-vegetation interaction

This series of parametric study considers cases with and without considering the VWC effects on microbial activity (i.e., $f_{V,m}$ in Eq. (A2)) upon plant root-water uptake. For cases that do not consider the VWC effects on microbial activity, mathematically the term $f_{V,m}$ was set to be 1.0 and independent on soil VWC. In these cases, only the effects of enhanced soil aeration by root-water uptake can be evaluated. In order to further highlight the importance of considering the coupled microbe-vegetation interaction, two types root architectures (uniform and exponential; refer to Fig. 1) and different root depths (ranged from 0.1 to 0.5 m) are selected for investigation. These two root architectures are chosen because they provide the largest contrast of VWC distributions among the four architectures (Ng et al., 2015a).

Table 2 Summary of parametric study

Series[a]	Case ID	Root architecture (refer to Fig. 1)	Root depth (m)	Transpiration rate (mm/day)
1[b]	RD1	Exponential and Uniform	0.1	4
	RD2		0.2	
	RD3		0.3	
	RD4		0.4	
	RD5		0.5	
2[c]	RA1	Exponential	0.3	4
	RA2	Triangular		
	RA3	Parabolic		
	RA4	Uniform		
3[c]	TP1	Exponential and Uniform	0.3	1
	TP2			2
	TP2.5			2.5
	TP3.3			3.3
	TP6.6			6.6

Note: (a) The duration considered for all cases is 34 days.

(b) Initial water contents of 17.2% is considered for series 1. Series 1 are analysed with and without consideration of the effects of soil water content on microbial activity.

(c) Two initial water contents of 17.2% and 36.8% are considered for both series 2 and 3. Analyses for bare soils are also performed for series 2 and 3, for control and comparison.

Figs 2(a), (c) and (e) show the distributions of VWC for the cases with root depths of 0.1, 0.3 and 0.5 m, respectively. Unless otherwise stated, all analyses with and without considering the VWC-dependency on microbial activities and all the results presented refers to the responses on Day 34 (i.e., at the end of analysis). As expected, significant reduction of VWC takes place mainly within the respective root zone due to root-water uptake upon transpiration. It can be seen that regardless of the root depths considered, uniformly-rooted soil always reduces VWC more significantly than exponentially-rooted soil within root zone. More detailed discussion on the effects of root architectures on VWC are given in the next section. The corresponding distribution of methane oxidation rate for each root depth case is depicted in Figs 2(b), (d) and (f). For shallow root depth of 0.1 m (Fig. 2(b)), a parabolic distribution of methane oxidation rate is found in all cases, when the dependency of VWC on microbial activity is ignored. No major difference is found between uniformly- and exponentially-rooted soils. The rate peaks at approximately 0.2 m depth. The peak methane oxidation rate takes place at deeps deeper than the root zone because the oxygen transfer in the vegetated soils has been improved by root-water uptake, allowing MAMO to be more easily taken place in deeper soil depths. This is consistent with the laboratory test data reported by Bohn et al (2011), Reichenauer et al. (2011), Hilger et al. (2000) and Wang et al., (2008). When VWC-dependency on microbial activity is considered, there is a significant reduction of the rate of MAMO within the root zone for both cases of uniform and exponential root architectures. This highlights the effects of water shortage of microbes caused by root-water uptake, following Eq. (A2). Below the root zone, there is almost no effect on the methane oxidation rate.

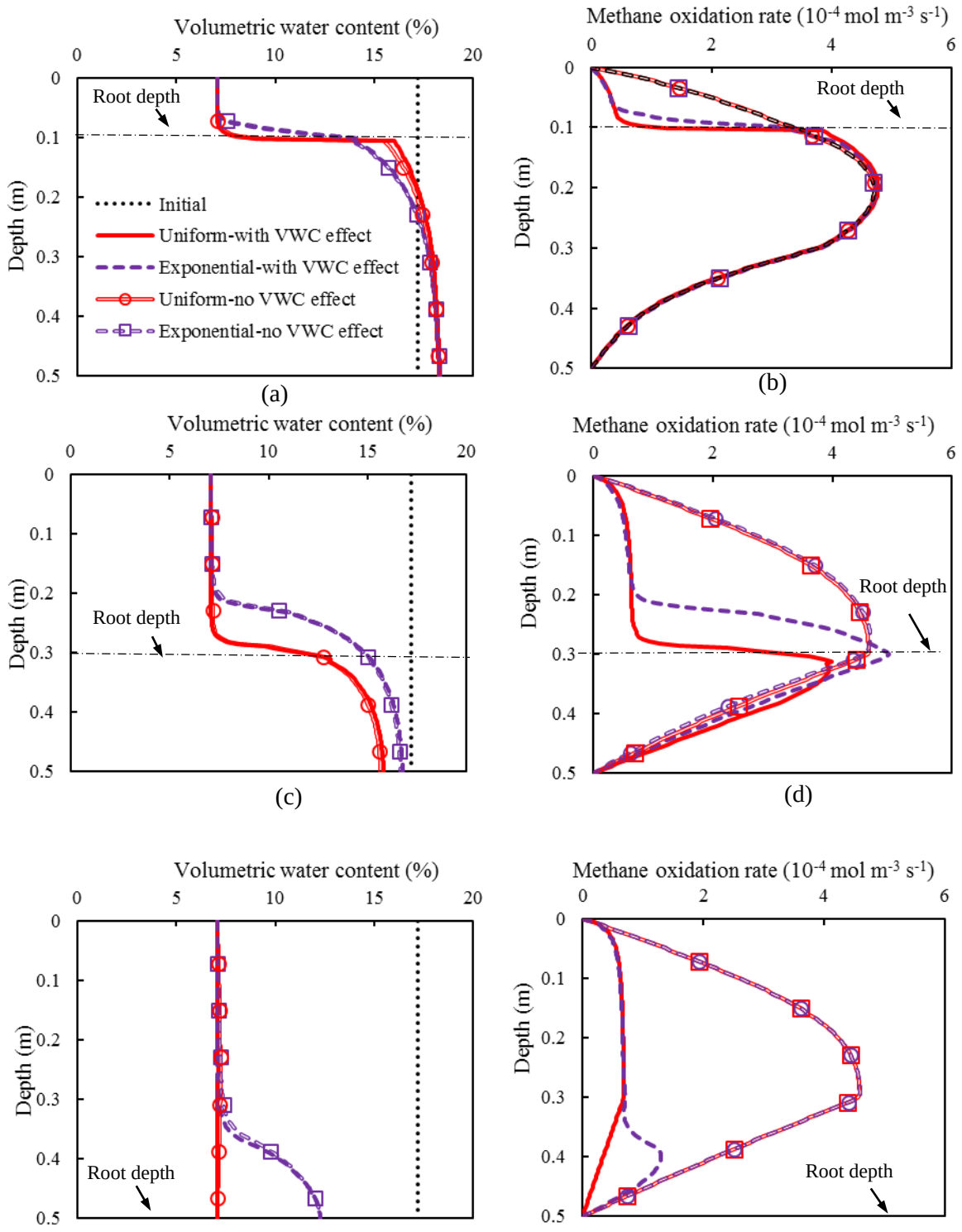

Figure 2 Distributions of volumetric water content ((a), (c), (e)) and methane oxidation rate ((b), (d), (f)) for root depths of 0.1, 0.3, and 0.5 m

The importance of the coupled microbe-vegetation interaction on MAMO becomes much more prominent when root depth increases, for both the root architectures considered. For deeper root depth of 0.3 m (Fig. 2(d)), the differences of methane oxidation rate for cases with and without considering VWC-dependency on microbial activity are much larger within the entire root zone. The over-prediction of the methane oxidation rate due to the negligence of the water shortage on microbes depends on the root architecture. It can be seen that the influence zone where the methane oxidation rate has been affected is smaller for the exponentially-rooted soil, because root-water uptake mainly concentrates on shallower depths (see Fig 2(c)).

Interestingly, without considering VWC-dependency on microbial activity, a further increase in root depth from 0.3 m (Fig 2(d)) to 0.5 m (Fig 2(f)) does not cause noticeable change in the entire profile of methane oxidation rate, regardless of the root architecture. This is because the difference of VWC profiles up to depth of 0.3 m between the cases with root depths of 0.3 and 0.5 m is less than 4% (see Figs 2(c) and 2(e)), leading to similar gas transfer and hence the rate of methane oxidation. While below depth of 0.3 m, it is expected that gas transfer is mainly affected by the applied constant upward influx of methane and carbon dioxide at the column base, resisting the downward inflow of oxygen from the atmosphere to the soil. Hence, this causes similar gas transfer and the rate of methane oxidation. On the contrary, when the effects of water shortage on microbial activity is taken into account, the increase in root length from 0.3 to 0.5 m could result in (1) an increased depth where the maximum methane oxidation rate takes place and (2) significant reduction of the magnitude of the peak methane oxidation rate, for both exponential and uniform cases.

Fig.3 shows the effects of root depth on MAMO efficiencies. When the effects of VWC on water shortage on microbe is ignored, the MAMO efficiencies for both uniformly- and exponentially-rooted soils rises only marginally to about 90% as root length increases. In contrast, when VWC-dependency on microbial activity is considered, the MAMO efficiencies in any case dropped significantly with an increase in root depth. This is because deeper roots create greater depth of water shortage for microbes to reduce their efficiency for MAMO. Despite the significant reduction of efficiency of both types of rooted soil, the exponentially-rooted soil is always more efficient than the uniformly-rooted soil, by up to 20%.

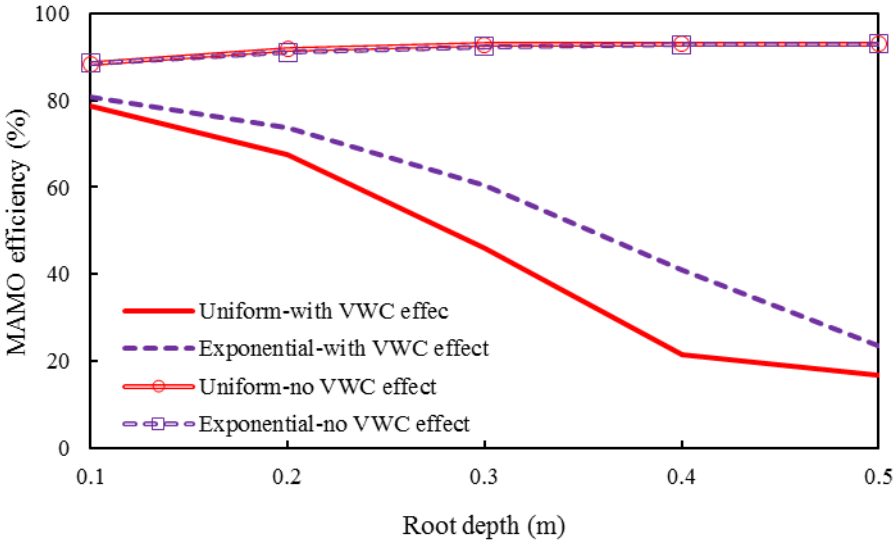

Figure 3 Effects of root depth on the coupled microbe-vegetation interaction on MAMO efficiency

The over-prediction of MAMO efficiency due to the negligence of the VWC-dependency of microbial activity increases with an increase in root depth. The maximum over-prediction found in this study could be as high as 75%. This highlights that for more correctly determining the MAMO efficiency of a rooted soil, it is important to consider the coupled effects of plant transpiration and microbial activity on water-gas flow.

3.2 Influence of root architecture

Fig. 4 (a) compares the VWC distributions between bare and vegetated soils when these soils are initially wet at plant anaerobiosis point. When vegetation is absent, there is a redistribution of VWC in the bare soil column due to downwards gravity-induced flow and the water generation by MAMO ($\rho_{DB}M_{H_2O}r_w$ in Eq. (1)) near the column base. The presence of vegetation, as expected, caused a larger reduction of VWC, especially within the root zone, due to root-water uptake. It can be seen that regardless of the root architectures, almost the same minimum VWC of 7% (i.e., θ_{wilt} in Eq. (9)) was found within the root zone. This is not surprising because it is the intention of this study to consider the same total root area among the four architectures (hence the volume of water transpired) for fair comparison (refer to Eq. (6)). Vegetated soil with exponential and triangular root architectures have nearly the same VWC distributions due to the similar root distributions (see Fig. 1 and refer to Eq. (6)). Indeed, when a deeper root depth of 2 m and the same β of 1 m^{-1} are considered, the root distribution between the exponential and triangular root architectures is much larger (Fig. S1(b); see Part 3 in SI). Hence, plant species that has exponential architecture induced lower VWC (see Fig. S2(a)) above depth of 0.5m, where MAMO mainly occurs, leading to lower methane oxidation rate (see Fig. S2(b)) due to the effects of water shortage on microbes. This is consistent with the analysis undertaken by Ng et al. (2015a), who also found that these two root architectures give a similar pore-water pressure distribution. On the other hand, uniform and parabolic rooted soils also have a similar VWC distribution, except near the column surface where a 3% difference in water content is observed. It can also be identified that outside the root zone, VWCs in the vegetated soils with uniform and

parabolic root architectures were lower than those in the cases of exponential and triangular, suggesting that the former two architectures induced a deeper depth of influence zone of VWC.

When the soil was initially dry at the initial VWC considered by De Visscher et al. (1999) (Fig. 4(b)), there is a uniform increase in VWC in bare case, which is in contrast to the non-uniform VWC distributions when the soil was initially wet. This is because drier soil has a lower water permeability, hence causing reduced downward water flow. As a result, the water generation by MAMO increased the VWC more uniformly for the initially dry case, as similarly observed in the numerical simulations performed by Molins et al. (2008) and Ng et al. (2015b). In this dry case, plant root-water uptake also caused a similar reduction of VWC to the minimum value of 7%, but the depth of influence (0.2 – 0.3 m) was considerably deeper than the wet case, regardless of the root architectures considered. Relatively speaking, the effects of root architecture on VWC distributions appear to be more prominent when the soil is initially wet. This is because for the dry case, the soil has already reached the threshold suction ψ_{ws} (refer to Eq. (5)), where plant has a reduced ability of water uptake for a given transpiration rate. The simulations suggest that plant species that have uniform or parabolic root architecture might have better water percolation control as they are more capable of recovering the water storage capacity of a wet landfill cover after subjecting to rainfall.

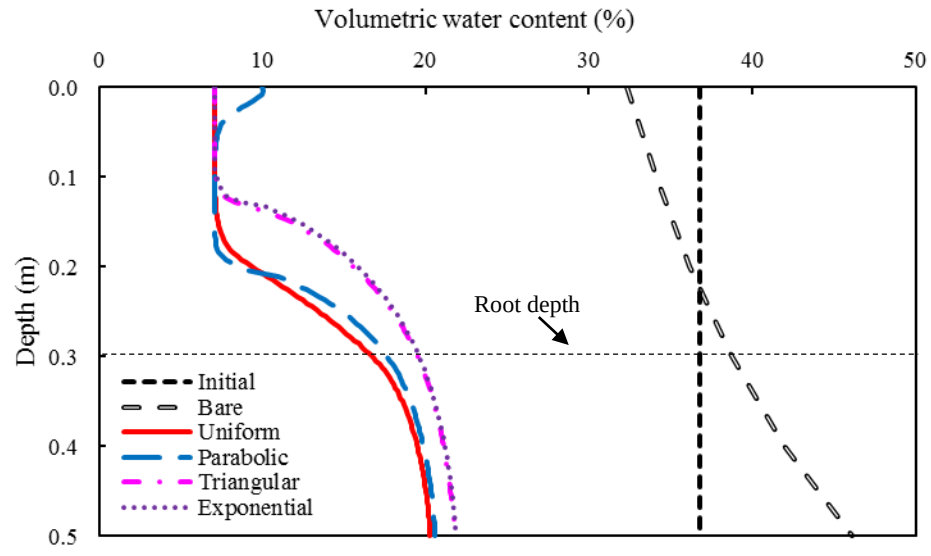

(a)

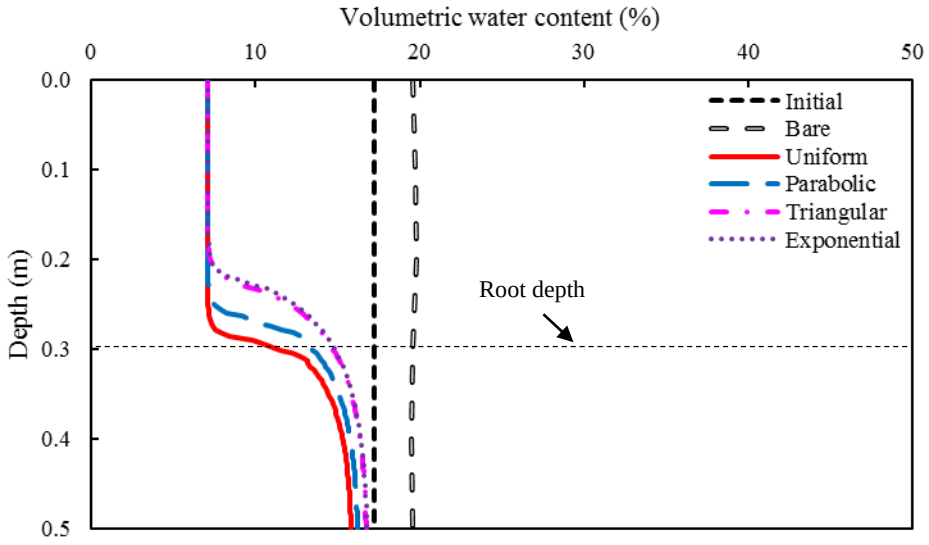

(b)

Figure 4 Effects of root architecture on the distributions of volumetric water content: (a) initially wet condition; and (b) initially dry condition

Fig. 5 (a) shows the effects of root architecture on the distributions of the ratio of methane (CH_4) to carbon dioxide (CO_2) under initially wet condition. A lower CH_4/CO_2 ratio suggests higher MAMO (Gebert et al., 2011; Einola et al., 2008). For the bare soil column, the aerobic depth (i.e., the depth up where the concentration of oxygen is negligible) reaches the depth of 0.2 m. On the

contrary, the aerobic depth of all vegetated columns is at the column base as a considerable concentration of oxygen is detected throughout the column. The much deeper aerobic depth observed in the vegetated soil is because of the improved soil aeration of oxygen transfer due to the reduction of VWC upon root-water uptake (refer to Fig. 4(a)). Enhanced soil aeration by vegetation is also reported in laboratory tests (Bohn et al, 2011; Reichenauer et al., 2011). Due to enhanced MAMO by the vegetation, the CH_4/CO_2 ratio in the vegetated soil (regardless of the root architectures) is significantly lower than that in the bare soil. The effects of root architecture on the CH_4/CO_2 ratio appear to be prominent mainly within the root zone. Among the four root architectures, the exponential and triangular ones yield almost the same lowest CH_4/CO_2 ratio and hence have higher MAMO.

The performance of MAMO of both the bare and vegetated soil columns is very much different when the process takes place in the initially dry condition (Fig. 5(b)). As expected, a deeper aerobic depth and a lower CH_4/CO_2 ratio are found for the bare soil column since the soil aeration, hence oxygen transfer, is better when the soil is dryer. In this dry case, the effects of root architecture on CH_4/CO_2 ratio are more significant compared with the wet case. Relatively speaking, the vegetated soils that have parabolic and uniform root architectures have higher CH_4/CO_2 ratio due to greater reduction of VWC by root-water uptake (Fig. 4(b)). Interestingly, when the soil is initially dry, the presence of vegetation (regardless of the root architecture) generally does not provide significant improvement of MAMO as the CH_4/CO_2 ratio of the bare soil, especially in shallower depths up to 0.2 m, is smaller than that of the vegetated soils. This is because, for the soil type and the dryness considered, the soil aeration (or gas permeability and diffusion) has already been high enough for significant MAMO to take place, without much need

of soil drying by vegetation. Furthermore, excessive soil moisture removal by roots in initially dry soil has induced water shortage on microbial activity.

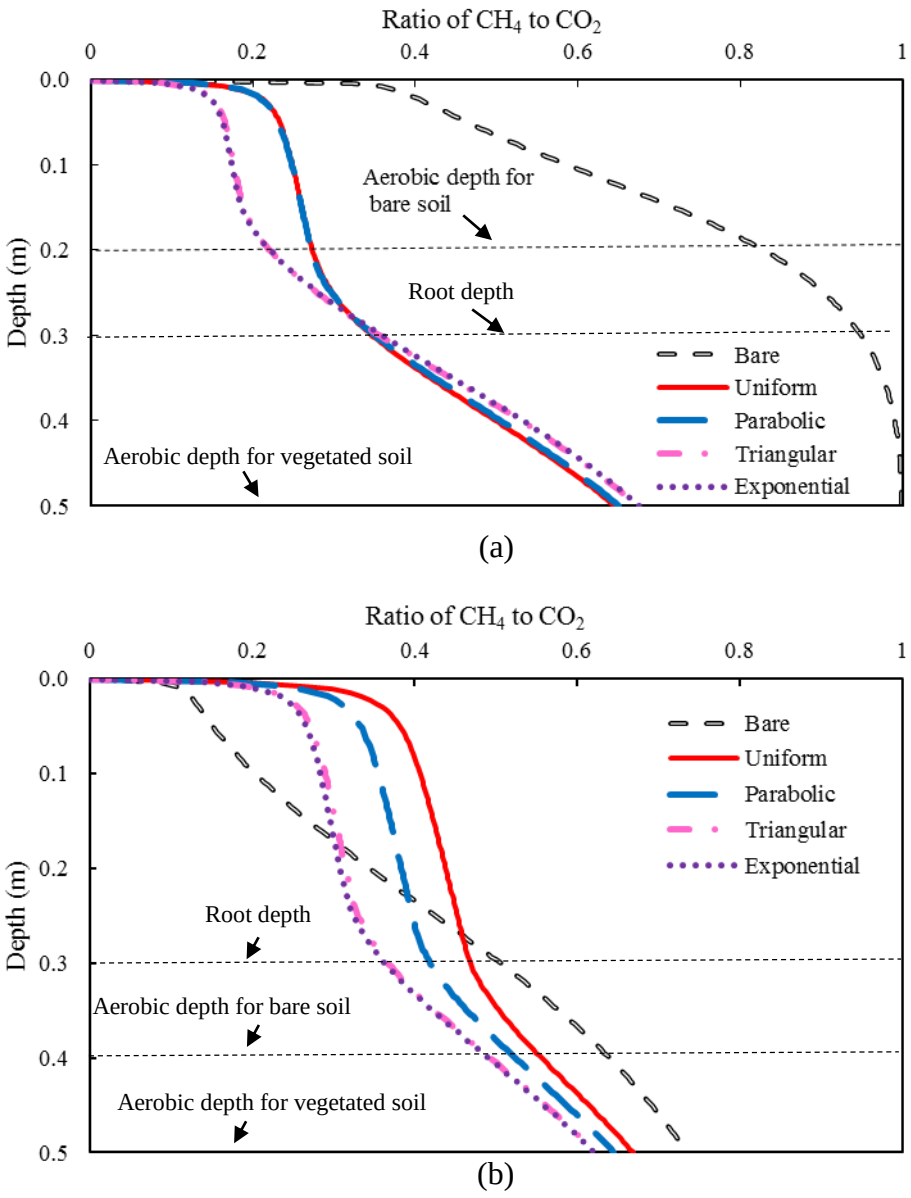

Figure 5 Effects of root architecture on the distributions of the ratio of methane (CH_4) to carbon dioxide (CO_2): (a) initially wet condition; (b) initially dry condition

Fig.6 (a) compares the MAMO efficiency between the bare and vegetated soils when the soil is initially wet. As expected, the bare soil has a nearly constant MAMO efficiency and maintains at about 50%. For the vegetated soils, regardless of the root architectures considered, there is a consistent linear increase in MAMO efficiency due to the continuous soil moisture removal by root-water uptake until Days 20 to 23 when a peak efficiency of 80 – 85% is found. The improvement of MAMO efficiency made by the vegetation has also been similarly observed in various experiments, especially when the vegetated soil was regularly irrigated to maintain high soil water content (Bohn et al, 2011; Reichenauer et al., 2011; Hilger et al., 2000; Wang et al., 2008). As plant transpiration takes place, the associated reduction of VWC reaches a threshold value, beyond which the amount of soil moisture would suppress the microbial activity (i.e., described by the term $f_{V,\mathrm{m}}$ in Eq. (A2)). This effect counteracted, and eventually dominated, the beneficial effects of the improvement of soil aeration brought by the root-water uptake, thus causing a reduction of the MAMO efficiency. The simulations also show that although the vegetated soil having a uniform or parabolic root architecture has higher peak MAMO efficiency, the reduction rate for these two cases are much more significant than the other two architectures. This is attributable to the greater reduction of VWC due to the greater ability of root-water uptake provided by the uniform and parabolic architectures (refer to Fig. 4 (a)), causing comparatively more significant water shortage for the microbial activity to take place.

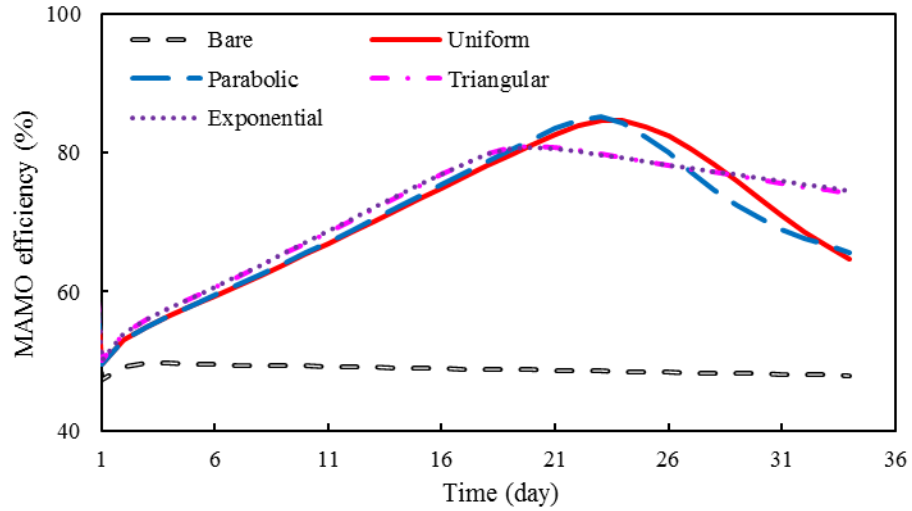

(a)

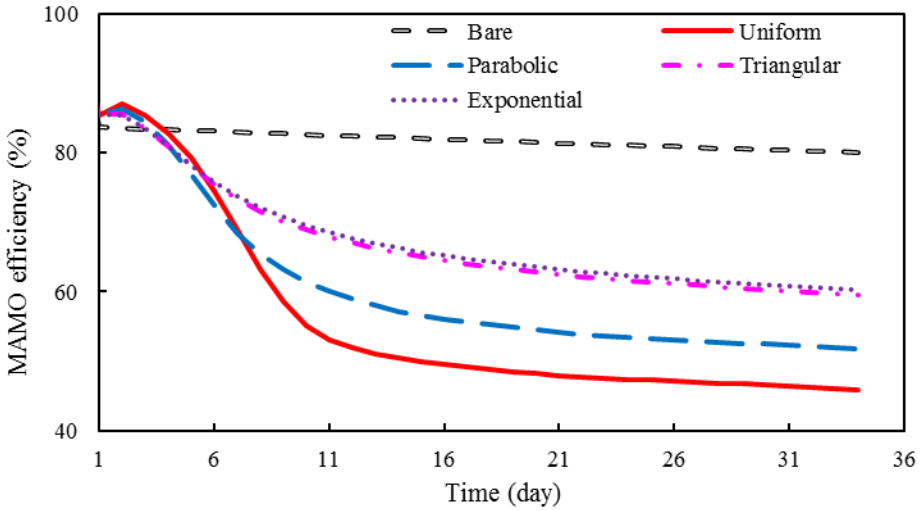

(b)

Figure 6 Effects of root architecture on MAMO efficiency: (a) initially wet condition; (b) initially dry condition

When the soil is initially dry, the presence of vegetation, however, has lower MAMO efficiency than the bare soil, for all four root architectures considered (Fig. 6 (b)). Since the VWC is low initially, further reduction via root-water uptake suppresses the microbial activity much earlier due to the quicker water shortage than the wet case. This thus causes a corresponding reduction of the MAMO efficiency to a level much lower than the bare soil (~83%), even in just the first few days of the no-rain period. The test results reported by Tanthachoon et al. (2008) also show that the bare soil has higher MAMO efficiency than vegetated soils when the soil was relatively dry without irrigation for 80 days. The observed greater reduction of the MAMO efficiency for the case of uniform root architecture is associated with its relatively strong ability of root-water uptake when compared to other architectures.

3.3 Influence of transpiration rate

The third series of parametric study evaluates the effects of plant transpiration rate (T_p in Eq. (4)), with due consideration of different climatic conditions and its interaction with plant water uptake. A range of transpirations from 1 to 6.6 mm/day (Leung et al., 2015) were selected to examine their effects on MAMO when soil is initially dry or wet. In this series, only uniform and exponential root architectures are considered for investigation.

Fig. 7(a) shows the effects of transpiration rate on η (Eq. (9)) along depth when the soil is initially wet. For the bare soil, η for the whole column is less than 1, indicating that poor soil aeration is the dominant mechanism that reduces MAMO. Vegetated soils, on the contrary, have

much higher η, especially within the root zone, due to the improvement of soil aeration by root-water uptake. It can be further observed that for a given root architecture, η increases with an increase in transpiration rate. When the transpiration rate is relatively low (2.5 mm/day), the plant root-water uptake, either with the exponential or uniform root architecture, is too weak to improve the soil aeration, as the values of η are always lower than 1.0 for the entire columns. As transpiration rate increases further, η within the root zone becomes higher than 1.0, suggesting that the MAMO is more affected by the microbial water shortage rather than the lack of oxygen transfer. Another interesting observation is that there seems to exist a threshold transpiration rate, beyond which the maximum η remains unchanged. It can be seen that at the soil surface, the η maintains at about 8 even the transpiration rate increases from 3.3 to 6.6 mm/day. It is because for any transpiration rate that exceeds 3.3 mm/day, the VWC at soil surface would have already reduced to the value corresponding to the permanent wilting point, beyond which both the plant root-water uptake and microbial activity stop.

When the soil is initially dry, the η of the vegetated soil appears to be less sensitive to the transpiration rate (see Fig. 7(b)) as compared to the previous case. For the case of uniform root architecture, almost the same profile of η is found for the three transpiration rates considered. Similar observation is found for the case of exponential root architecture, except at 0.2 m depth where the root-water ability reduces according to Eq. (5). Based on η at soil surface, the threshold transpiration rate in this dry case appears to be 2.5 mm/day, which is lower than that identified in the wet case in Fig. 7(a). This is because when the soil is drier, less amount of transpiration is needed to reduce VWC to the value corresponding to the permanent wilting point.

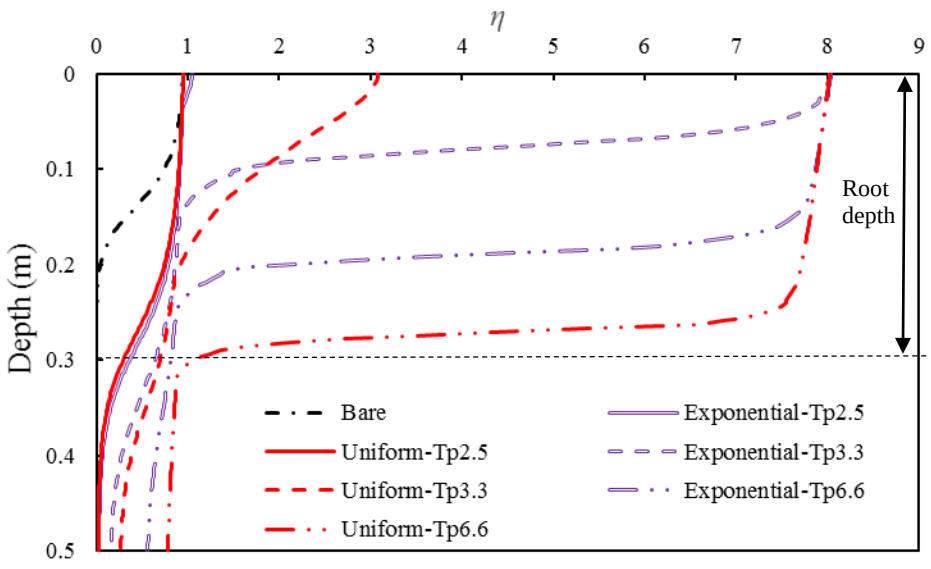

(a)

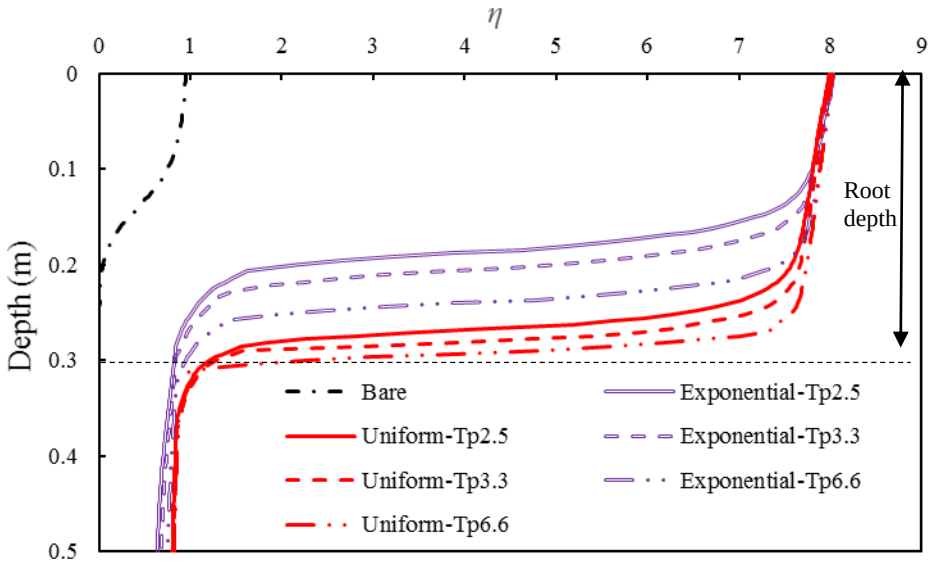

(b)

Figure 7 Effects of transpiration rate on η (the ratio of f_{O2} to $f_{V,m}$) along depth: (a) initially wet condition; (b) initially dry condition

Fig. 8(a) shows the effects of transpiration rate on MAMO efficiency when the soil is initially wet. The water shortage coefficient, ϖ (Eq. (10)), corresponding to each transpiration rate is

584 also depicted. The bare soil has a constant coefficient of 48%. On the contrary, an increase in
585 plant transpiration rate improves the aeration in vegetated soils and this hence increases MAMO
586 efficiency. The increasing rate of the efficiency appears to be independent of the root
587 architecture. The vegetation improves MAMO efficiency only until the ϖ reaches 1.0, beyond
588 which the soil VWC would be too low to meet the demand of root-water uptake. When
589 transpiration rate increases further, the continuous loss of VWC has an adverse effect to MAMO
590 efficiency as the MAMO has been predominantly suppressed by the water shortage of microbes.
591 Since the η of the uniformly-rooted soil is higher than that of the exponentially-rooted soil (Fig.
592 7(a)), the reduction rate of the MAMO efficiency for the former case is thus more significant.
593
594 When the soil is initially dry (Fig. 8(b)), the MAMO efficiency of bare soil (i.e., 80%) is higher
595 than the initially wet case, as expected, due to better soil aeration. For vegetated soils, it is
596 interesting to see that even at a low transpiration rate of 1 mm/day, the ϖ has already reached
597 1.0, meaning that the plants find them difficult to extract water from the relatively dry soil. A
598 further increase in transpiration rate hence results in greater shortage of water for microbes to
599 undergo MAMO, consequently reducing the efficiency. Consistent with the findings from the
600 wet case in Fig. 8(a), the efficiency reduction rate for the uniformly-rooted soil is much more
601 significant than that for the exponentially-rooted soil. It appears that for the uniformly-rooted soil,
602 transpiration rate of about 3 mm/day is the threshold value, beyond which the plant root-water
603 uptake does not play any further role on MAMO efficiency.
604

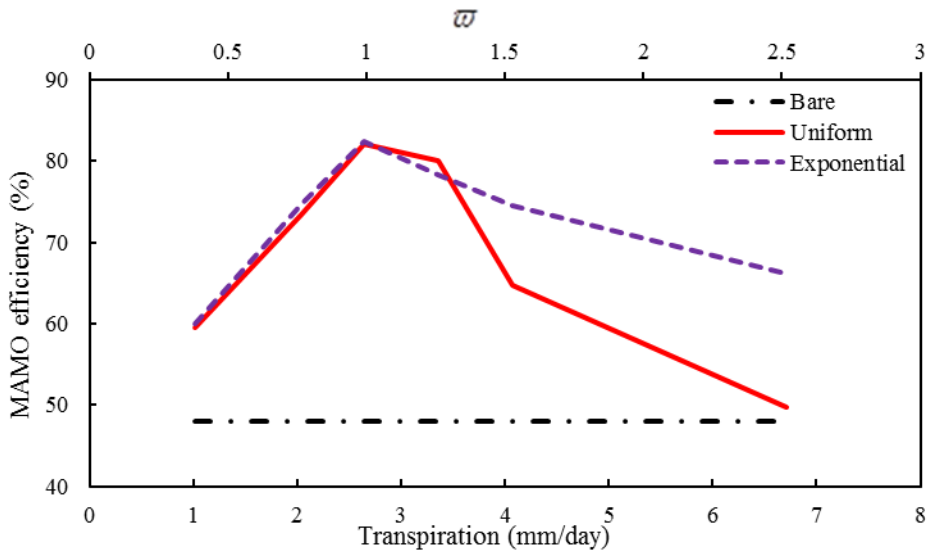

(a)

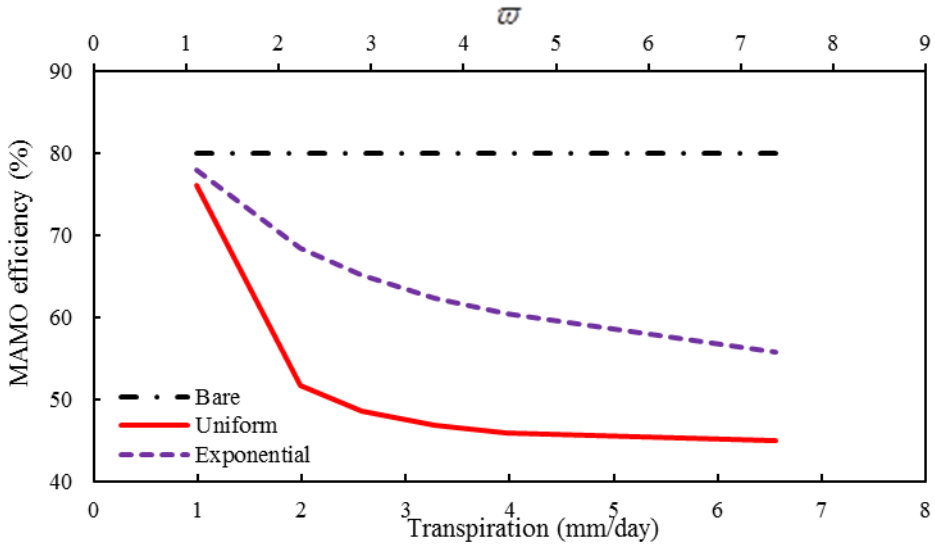

(b)

Figure 8 Effects of transpiration rate on MAMO efficiency: (a) initially wet condition; (b) initially dry condition

3.4 Engineering implications

It is clear from the simulation that MAMO is a complex process where the interplay among the initial soil moisture condition, ability of root water take and climate condition could cause shifts of the significance of soil aeration and microbial water shortage on MAMO efficiency. Among

616 the plant root architectures considered, exponential/triangular root architectures are more
617 preferable and they appear to perform better in terms of MAMO efficiency than
618 uniform/parabolic one. At high transpiration rate of 5 mm/day, MAMO efficiency for the
619 exponentially-rooted soil that is initially dry can be even higher than the uniformly-rooted soil
620 that is initially wet (Fig. 8(b)). Planting vegetation that has exponential/triangular root
621 architectures have additional benefit to the sloping part of a landfill, as these two root
622 architectures have greater stabilization effects on shallow slope stability compared to
623 uniform/parabolic ones (Ng et al., 2015a; Liu et al., 2016).
624
625 The simulation reveals that if a landfill cover is to be built at arid or semi-arid regions where the
626 soil remains relatively dry, special attention should be paid to the emission of methane gas as the
627 presence of vegetation could demote the microbial activity for MAMO. In particular, water
628 uptake by plant species that has triangular/exponential root architectures introduced less water
629 shortage on microbes and hence less reduction in MAMO efficiency (see Figs. 3 and 6).
630 However, it is important to highlight that these root architectures are not ideal in terms of water
631 percolation, which is another important aspect that should not be overlooked for the design of
632 landfill cover. In fact, plants with uniform and parabolic root architectures and relatively long
633 root depth provide better hydrological performance because these root architectures have greater
634 water uptake ability to reduce soil water content and hence hydraulic conductivity. In contrast,
635 for landfill covers to be built in humid regions where soil is normally wet, the choice of root
636 architecture may be less critical because microbes are less likely to have water shortage for
637 oxidizing methane even root-water uptake takes place. A careful assessment of site climate is
638 thus crucial for landfill designers to judge whether methane gas emission, water percolation or

639 their combination is controlling the design of landfill cover before plant species with desirable
640 characteristics is selected.
641
642 Another important engineering implication to landfill designers is that plants with different root
643 depths and root architectures require different irrigation schedule (refer to Fig. 3). For a given
644 root architecture, a more frequent irrigation may be needed for deeper root case, which the drop
645 of MAMO efficiency is more significant. This implies that for a longer term vegetation
646 management of a landfill cover, the frequency of irrigation schedule should be generally
647 increased as roots grow to deeper depths. For a given root length, plant species that has uniform
648 or parabolic root architectures may require more frequent irrigation than the exponential and
649 triangular ones, because the former two introduced greater water shortage on microbes due to
650 their greater ability of water uptake. For the specific conditions considered in this study (Fig. 4),
651 up to 15% more water was needed for both the uniform and parabolic cases to maintain the same
652 MAMO efficiencies as the other two cases. Nonetheless, regardless of the length or architecture
653 of roots considered, any enhanced percolation due to the formation of soil macro-pores upon root
654 growth/penetration (Beven and Germann, 1982) has to be carefully assessed, with due
655 consideration of root architecture and weather forecasting of precipitation. No excessive water
656 should be added to result in decreased MAMO by reducing oxygen availability.
657
658 The dimensionless ratio, η, might be a relevant indicator for landfill operators to make a more
659 objective decision on the need of irrigation, if monitoring of volumetric fraction of oxygen (i.e.,
660 y_{O_2} in Eq. (9)) and soil water content in shallow soil (0.5~1 m) were available. Soil water content
661 data could be used to determine $f_{V,m}$ via Eq. A2, while f_{O_2} could be obtained by measured y_{O_2}

and considering K_{O_2} to be 0.012 (based on the direct measurements reported by De Visscher et al. (1999)). Hence, η could be estimated via Eq. (9). If η is higher than 1.0 (i.e., MAMO being suppressed by microbial activity), irrigation may be applied.

4 Conclusions

This study proposes a newly-improved theoretical model that couples the effects of plant root-water uptake and microbial activity for more realistically capturing water-gas flow and microbial aerobic methane oxidation (MAMO) in unsaturated soils. Another new feature of the model is to allow for consideration the effects of different root architectures, namely uniform, parabolic, exponential and triangular, on MAMO.

The simulation shows that ignoring the effects of water shortage on microbes (like most of the existing models do) would over-predict the MAMO efficiency in vegetated soils, especially when the plant has a uniform root architecture. The over-prediction would be magnified when root depth is deeper (i.e., greater soil volume being effected by root-water uptake), because the water shortage on microbes is much more prominent.

Plants with exponential and triangular root architectures and relatively short root depth are more preferable for maximizing the beneficial effects of root-water uptake on the control of methane gas emission from a landfill cover.

Whether the presence of plants is beneficial or adverse to methane gas emission control depends on the initial soil moisture and transpiration rate strongly. When the soil is initially wet at plant

anaerobiosis point, root-water uptake improves soil aeration within the root zone significantly, hence providing improvement on the MAMO efficiency. On the contrary, when the soil is initially dry near the permanent wilting point, plant root-water uptake, for any root architecture considered, reduces the MAMO efficiency as compared to bare soil. This is because when the soil is too dry, further reduction of soil moisture by plants would significantly suppress the microbial activity. Hence, this reduces the rate and efficiency of MAMO.

In order to further verify the proposed theoretical model, more comprehensive field or laboratory dataset is needed to quantify the combined effects of plants and microbes on methane oxidation efficiency. More research on how the presence of plant roots would cause any change in water and gas flow properties of unsaturated soil will be valuable. This information will improve the theoretical soil-root interaction models, which can gain further insights into the control of water percolation of a vegetated landfill cover.

Acknowledgements

The authors would like to acknowledge research grants (HKUST6/CRF/12R) provided by the Research Grants Council (RGC) of the Hong Kong Special Administrative Region. The second author acknowledges the EU Marie Curie Career Integration Grant under the project ‘BioEPIC slope’ and research travel support from the Northern Research Partnership (NRP).

Notation

ρ_w	water density
ρ_{DB}	dry bulk density of soil
M_{H_2O}	molar mass for water
r_w	generation rate by per mole methane oxidation
θ_w	volumetric water content
θ_{sat}	saturated volumetric water content
θ_{wilt}	wilting point of soil
θ_{fc}	field capacity of soil
v_w	velocity of Darcian water flow
$S(\psi, z)$	sink term associated with plant root-water uptake as a function of matric suction
ψ	matric suction
z	depth
H(z)	Heaviside function
P_g	gas pressure
P_w	pore-water pressure

721 L_1 length outside the root zone

722 L_2 root depth

723 g gravitational acceleration

724 k_w water permeability function

725 T_p transpiration rate

726 $\alpha(\psi)$ transpiration reduction function

727 ψ_{os} anaerobiosis point

728 ψ_{ws} turning point

729 ψ_{wilt} the suction at wilting point

730 $G(z)$ root shape function describing root architecture

731 β a constant with a unit of m^{-1}, which controls the curvature of exponential root architecture

732 V_{max} maximum methane oxidation rate per unit mass of dry soil

733 K_m half saturation constants for methane

734 Ko_2 half saturation constants for oxygen

735 y_{CH_4} molar fraction of methane

736 y_{O_2} molar fraction of oxygen

737 $f_{V,T}$ effect of temperature on microbial activity

738 $f_{V,m}$ effect of water content on microbial activity

739 f_{O_2} the effects of root-water uptake on the improvement of soil aeration

740 η dimensionless number defined as $f_{O_2} / f_{V,m}$

741 θ_{wilt} volumetric water content at wilting point

742 θ_{ini} initial volumetric water content

743 ϖ water shortage coefficient defined as $T_p * t/(\theta_{wilt} - \theta_{ini})r_d$

744 t time

745 T_p maximum root-water uptake

746 $\Gamma_{CH_4}^{in}$ methane influx

747 $\Gamma_{CH_4}^{out}$ methane outflux

748 η_{oxi} MAMO efficiency

749 ϕ soil porosity

750 S_w degree of saturation

751 c_g^k molar concentration of gas *k*

752 H_w^k molar concentration of gas *k* dissolved in water

753 v_g advective velocity of the gas mixture

754 N_g^k diffusive flux of gas *k* in the gaseous phase

755 r_g^k reaction rate per unit of dry soil mass for gas *k*

756 $r_g^{CH_4}$ MAMO rate

757 T soil temperature

758

References

Abichou, T., Mahieu, K., Chanton, J., Romdhane, M. and Mansouri, I. (2011). Scaling methane oxidation: from laboratory incubation experiments to landfill cover field conditions. Waste Management, 31, 978–986.

Abichou, T., Kormi, T., Yuan, L., Johnson, T. and Francisco, E. (2015). Modeling the effects of vegetation on methane oxidation and emissions through soil landfill final covers across different climates. Waste Management, 36, 230-240.

Beven, K. and Germann, P. (1982). Macropores and water flow in soils. Water Resources Research, 18(5), 1311-1325.

Bohn, S., Brunke, P., Gebert, J. and Jager, J. (2011). Improving the aeration of critical fine-grained landfill top cover material by vegetation to increase the microbial methane oxidation efficiency. Waste management, 31(5), 854-863.

Czepiel P, Mosher B, Crill P and Harriss R (1996). Quantifying the effect of oxidation on landfill methane emissions. Journal of Geophysical Research, 101, 16721–9.

De Visscher A and Van Cleemput O (2003). Simulation model for gas diffusion and methane oxidation in landfill cover soils. Waste Management, 23, 581–91.

De Visscher, A., Thomas, D., Boeckx, P. and Van Cleemput, O. (1999). Methane oxidation in simulated landfill cover soil environments. Environmental Science and Technology, 33, 1854–1859.

778 Einola, J. K., Sormunen, K. M. and Rintala, J. A. (2008). Methane oxidation in a boreal climate
779 in an experimental landfill cover composed from mechanically–biologically treated waste.
780 Science of the total environment, 407(1), 67-83.

781 Feddes, R.A., Kowalik, P., Kolinska-Malinka, K. and Zaradny, H. (1976). Simulation of field
782 water uptake by plants using a soil water dependent root extraction function. Journal of
783 Hydrology, 31 (1), 13–26.

784 Feng, S. (2016). Constitutive modelling of coupled bio-chemo-hydro-thermal reactive transport
785 considering methane oxidation and vegetation. PhD thesis, Hong Kong University of
786 Science and Technology, Hong Kong.

787 Feng, S., Leung, A.K., Ng, C.W.W. and LIU, H.W. (2017). Numerical modelling of methane
788 oxidation efficiency and coupled water-gas-heat reactive transfer in a sloping landfill
789 cover. Waste Management, provisionally accepted.

790 Gebert, J., Röwer, I. U., Scharff, H., Roncato, C. D. and Cabral, A. R. (2011). Can soil gas
791 profiles be used to assess microbial CH_4 oxidation in landfill covers?. Waste
792 Management, 31(5), 987-994.

793 Hilger, H. A., Wollum, A. G. and Barlaz, M. A. (2000). Landfill methane oxidation response to
794 vegetation, fertilization, and liming. Journal of Environmental Quality, 29(1), 324-334.

795 Hong Kong Observatory (2016). Daily total rainfall (mm) at the Hong Kong International
796 Airport. Hong Kong Observatory, Kowloon.
797 http://www.weather.gov.hk/cis/data/drf_summary_e.htm (accessed 9 Mar. 2016).

798 Kamchoom, V., Leung, A. K. and Ng, C. W. W. (2014). Effects of root geometry and
799 transpiration on pull-out resistance. Geotechnique Letters, 4(1), 330-336.

800 Leung, A. K. and Ng, C. W. W. (2013). Analyses of groundwater flow and plant
801 evapotranspiration in a vegetated soil slope. Canadian Geotechnical Journal, 50(12),
802 1204-1218.

803 Leung, A.K., Garg, A. and Ng, C.W.W. (2015). Effects of plant roots on soil-water retention and
804 induced suction in vegetated soil. Engineering Geology, 193, 183-197.

805 Leung, A. K., Kamchoom, V. and Ng, C. W. W. (2016). Influences of root-induced soil suction
806 and root geometry on slope stability: a centrifuge study. Canadian Geotechnical Journal,
807 available online.

808 Liu, H. W., Feng, S. and Ng, C. W. W (2016). Analytical analysis of hydraulic effect of
809 vegetation on shallow slope stability with different root architectures. Computers and
810 Geotechnics, 80, 115-120.

811 Molins S, Mayer KU, Scheutz C and Kjeldsen P (2008). Transport and reaction processes
812 affecting the attenuation of landfill gas in cover soils. Journal of Environmental Quality,
813 37(2), 459–68.

814 Mualem, Y. (1976). A new model for predicting the hydraulic conductivity of unsaturated porous
815 media. Water Resource Research, 12, 513–522.

816 Ng, C. W. W., Liu, H. W. and Feng, S. (2015a). Analytical solutions for calculating pore-water
817 pressure in an infinite unsaturated slope with different root architectures. Canadian
818 Geotechnical Journal, 52(12), 1981-1992.

819 Ng, C. W. W., Feng, S. and Liu, H. W. (2015b). A fully coupled model for water–gas–heat
820 reactive transport with methane oxidation in landfill covers. Science of The Total
821 Environment, 508, 307-319.

822 Ng, C. W. W., Kamchoom, V. and Leung, A. K. (2016). Centrifuge modelling of the effects of
823 root geometry on transpiration-induced suction and stability of vegetated slopes.
824 Landslides, 13(5), 925-938.

825 Nyambayo, V.P. and Potts, D.M. (2010). Numerical simulation of evapotranspiration using a
826 root water uptake model. Computers and Geotechnics, 37(1–2): 175–186.

827 Prasad, R. (1988). A linear root water uptake model. Journal of Hydrology, 99(3): 297–306.

828 Reichenauer, T. G., Watzinger, A., Riesing, J. and Gerzabek, M. H. (2011). Impact of different
829 plants on the gas profile of a landfill cover. Waste management, 31(5), 843-853.

830 Scheutz, C., Bogner, J., De Visscher, A., Gebert, J., Hilger, H., Huber-Humer, M., Kjeldsen, P.
831 and Spokas, K. (2009). Microbial methane oxidation processes and technologies for
832 mitigation of landfill gas emissions. Waste Management & Research, 27:409–55.

833 Spokas K and Bogner J. Limits and dynamics of methane oxidation in landfill cover soils (2011).
834 Waste Management, 31(5), 823–32.

835 Stein, V. B., Hettiaratchi, J. P. A. and Achari, G. (2001). Numerical model for biological
836 oxidation and migration of methane in soils. Practice Periodical of Hazardous, Toxic, and
837 Radioactive Waste Management, 5(4), 225-234.

838 Tanthachoon, N., Chiemchaisri, C., Chiemchaisri, W., Tudsri, S. and Kumar, S. (2008). Methane
839 oxidation in compost-based landfill cover with vegetation during wet and dry conditions
840 in the tropics. Journal of the Air & Waste Management Association, 58(5), 603-612.

841 Thomas, H. R. and He, Y. (1995). Analysis of coupled heat, moisture and air transfer in a
842 deformable unsaturated soil. Géotechnique, 45(4), 677-689.

843 Thomas, H. R. and Ferguson, W. J. (1999). A fully coupled heat and mass transfer model
844 incorporating contaminant gas transfer in an unsaturated porous medium. Computers and
845 Geotechnics, 24(1), 65-87.

846 USDA (1998). Keys to Soil Taxonomy. 8th edition. U.S. Department of Agriculture and Natural
847 Resource Conservation Service, U.S. Government Printing Office, Washington, DC,
848 USA.

849 Van Genuchten, M. T. (1980). A closed form equation for predicting the hydraulic conductivity
850 of unsaturated soils. Soil Science Society of America Journal, 44, 892–898.

851 Wang, Y., Wu, W., Ding, Y., Liu, W., Perera, A., Chen, Y. and Devare, M. (2008). Methane
852 oxidation activity and bacterial community composition in a simulated landfill cover soil
853 is influenced by the growth of Chenopodium album L. Soil Biology and Biochemistry,
854 40(9), 2452-2459.

855 Zhang, Y., Zhang, H., Jia, B., Wang, W., Zhu, W., Huang, T. and Kong, X. (2012). Landfill CH_4
856 oxidation by mineralized refuse: Effects of NH_4^+-N incubation, water content and
857 temperature. Science of the total environment, 426, 406-413.

858 Zhang, H., Yan, X., Cai, Z. and Zhang, Y. (2013). Effect of rainfall on the diurnal variations of
859 CH_4, CO_2, and N_2O fluxes from a municipal solid waste landfill. Science of the Total
860 Environment, 442, 73-76.

861

Tables and figures in the manuscript

List of tables in the manuscript

List of figures in the manuscript

The supplementary information includes:

Part 1 Formulations for considering the effects of temperature and water content on microbial activity

Part 2 Governing equation for multi-component gas transfer

Part 3 Extra figures

Figure S1 Four idealized root architectures: (a) at root depth of 1 m; and (b) at root depth of 2 m

Figure S2 Comparisons of the distributions of (a) VWC and (b) methane oxidation rate between triangular and exponential root architectures at root depth of 2 m

Supplementary Information

Theoretical analysis of coupled effects of microbe and root architecture on methane oxidation in vegetated landfill covers

S. Feng, A.K. Leung, C. W. W. Ng and H.W. Liu*,

Department of Civil and Environmental Engineering, Hong Kong University of Science and Technology, Clear Water Bay, Kowloon, Hong Kong

* (Corresponding author) **Address:** Department of Civil and Environmental Engineering, Hong Kong University of Science and Technology, Clear Water Bay, Kowloon, Hong Kong **E-mail:** hliuan@connect.ust.hk **Tel.:** +852 6849 4779

The supplementary material includes:

Part 1 Formulations for considering the effects of temperature and water content on microbial activity

Part 2 Governing equation for multi-component gas transfer

Part 3 Extra figures

Figure S1 Four idealized root architectures: (a) at root depth of 1 m; and (b) at root depth of 2 m

Figure S2 Comparisons of the distributions of (a) VWC and (b) methane oxidation rate between triangular and exponential root architectures at root depth of 2 m

Part 1. Formulations for considering the effects of temperature and water content on microbial activity

Effects of temperature on microbial activity ($f_{V,T}$) may be described by the following empirical expression proposed by Abichou et al. (2011):

$$f_{V,T} = \begin{cases} 2.235 - 0.18(T - 33) & T \geq 33\ ^{0}\text{C} \\ 0.122T - 1.47 & 15\ ^{0}\text{C} \leq T < 33\ ^{0}\text{C} \\ 0.0142T & T < 15\ ^{0}\text{C} \end{cases} \quad \text{(A1)}$$

where T is soil temperature. The physical meaning of Eq. (A1) is that below the optimum temperature of 33 ^{o}C, the rate of methane oxidation increases with an increase in temperature, but it is the opposite when soil temperature is higher than the optimum value. As a first approximation, the effects of soil water content on microbial activity ($f_{V,m}$) may be described by the following relationship proposed by (Abichou et al., 2011):

$$f_{V,m} = \begin{cases} 0 & \theta_w \leq \theta_{wilt} \\ \dfrac{\theta_w - \theta_{\text{wilt}}}{\theta_{fc} - \theta_{wilt}} & \theta_{wilt} < \theta_w \leq \theta_{fc} \\ 1 & \theta_{fc} < \theta_w \leq \theta_{sat} \end{cases} \quad \text{(A2)}$$

where θ_{sat} is the saturated volumetric water content; θ_{wilt} is the wilting point of soil, which is the water content when microbial activity for methane oxidation is negligible; and θ_{fc} is the field capacity of soil, and it is defined as the water content at which a soil can hold when drainage driven by gravity is negligible. Eq. (A2) describes that when soil water content is lower than θ_{wilt} , methane oxidation is negligible. As soil water content increases from θ_{wilt} to θ_{fc} , methane oxidation rate increases linearly to the maximum value. When the water content is higher than field capacity, $f_{V,m}$ becomes constant, meaning that the soil water content has no effect on

microbial activity. As a first approximation, θ_{wilt} to θ_{fc} maybe estimated by water content at suction of 40 and 1500 kPa (Feddes et al., 1976), respectively. This relationship is consistent with the datasets reported by Spokas and Bonger (2011), which is one of the very scarce studies that experimentally quantify relationship between methane oxidation rate and suction in the literature. Their test results show that the maximum and minimum methane oxidation rates occur at suction about 50 kPa (close to field capacity 33 kPa) and wilting point (1500 kPa), respectively. Beyond the wilting point, MAMO is found to be practically negligible. Therefore, as the first attempt to model the coupled effects and interaction between plant and microbes, application of the relationship found by Spokas and Bonger (2011) in our proposed model is deemed acceptable.

Part 2. Governing equation for multi-component gas transfer

Using a similar approach as Thomas and He (1995), invoking the principle of mass conservation for gas *k* yields

$$\frac{\partial}{\partial t}[(1-S_w)\phi c_g^k + S_w \phi H_w^k] = -\nabla[v_g c_g^k] - \nabla[v_w H_w^k] - \nabla N_g^k \pm \rho_{DB} r_g^k \qquad \text{(A3)}$$

where ϕ and S_w is the soil porosity and degree of saturation, respectively; c_g^k is the molar concentration of gas *k* (k = 1,2,3,4 represent O_2, CO_2, CH_4 and N_2, respectively); H_w^k is the molar concentration of gas *k* dissolved in water; v_g and N_g^k are the advective velocity of the gas mixture and the diffusive flux of gas *k* in the gaseous phase, respectively; r_g^k is the reaction rate

per unit of dry soil mass for gas *k*. Eq. (A3) considers that the transfer mechanisms of each gas component include (i) advection in the gaseous phase; (ii) advection of the dissolved gas *k* in water and (iii) gas diffusion in the gaseous phase.

Part 3 Supplementary figures

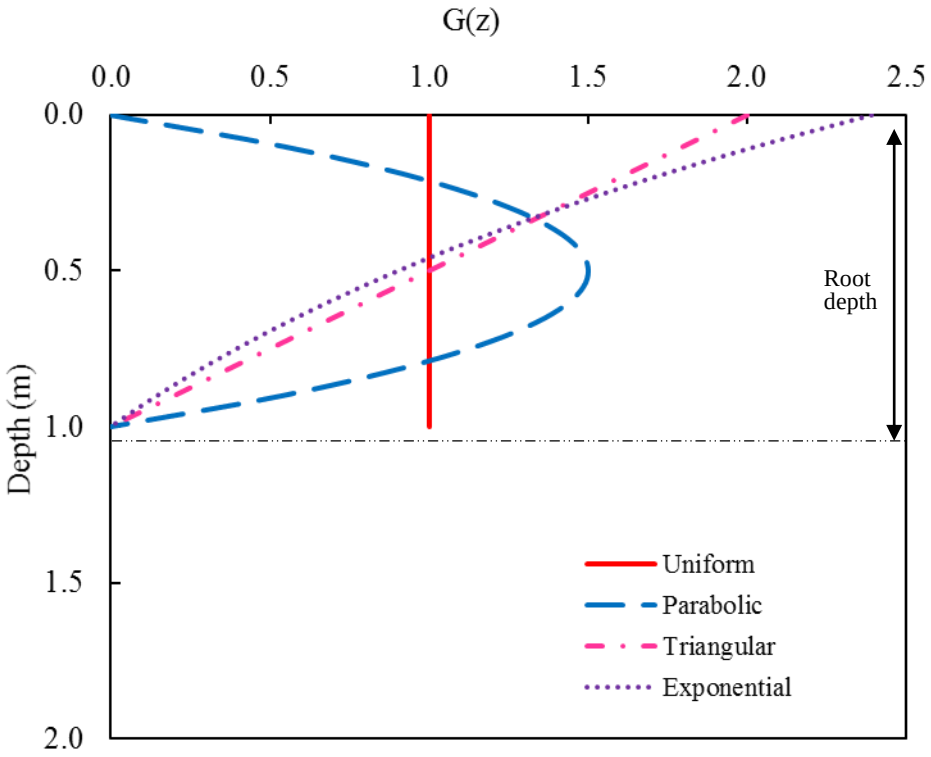

(a)

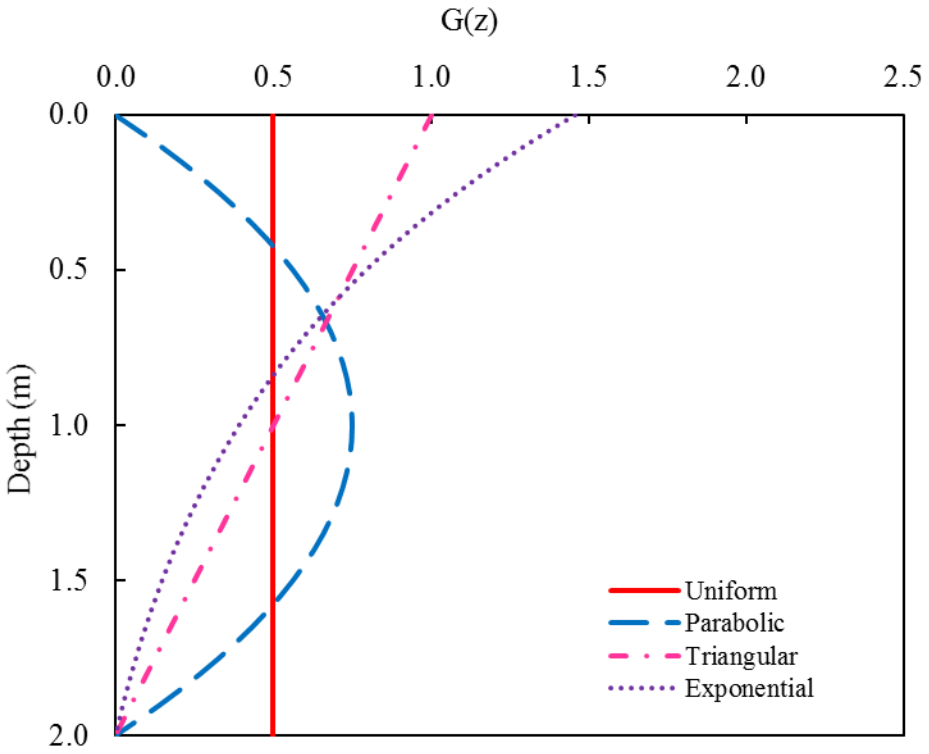

(b)

Figure S1 Four idealized root architectures: (a) at root depth of 1 m; and (b) at root depth of 2 m

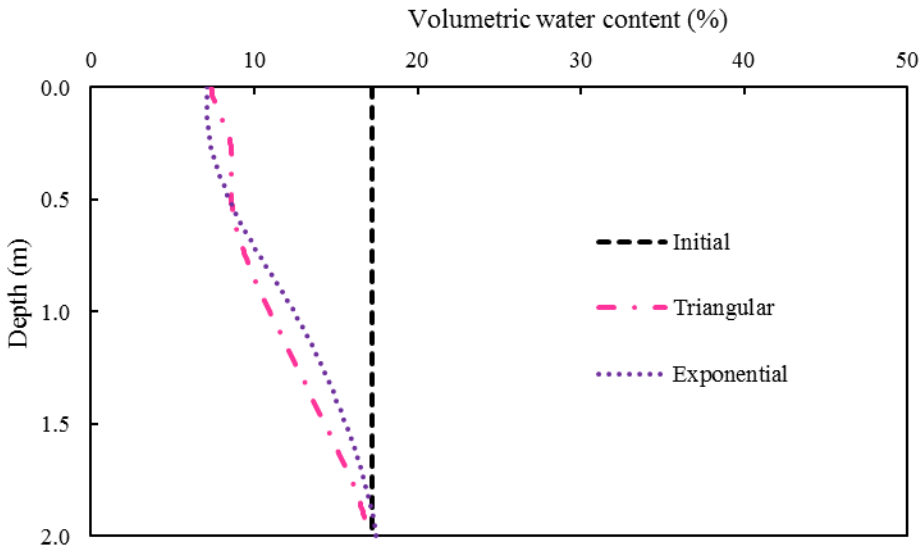

(a)

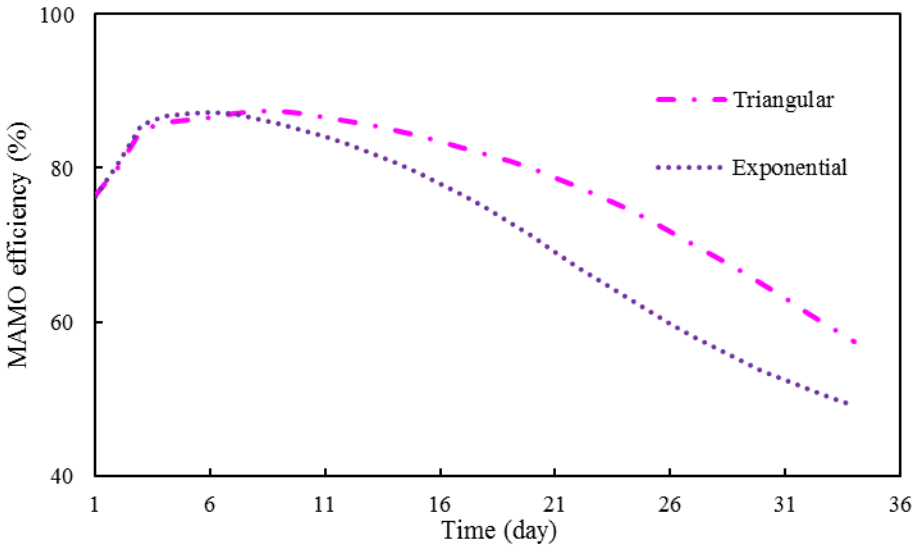

(b)

Figure S2 Comparisons of the distributions of (a) VWC and (b) methane oxidation rate between triangular and exponential root architectures at root depth of 2 m

References

Abichou, T., Mahieu, K., Chanton, J., Romdhane, M. and Mansouri, I. (2011). Scaling methane oxidation: from laboratory incubation experiments to landfill cover field conditions. Waste Management, 31, 978–986.

Feddes, R.A., Kowalik, P., Kolinska-Malinka, K. and Zaradny, H. (1976). Simulation of field water uptake by plants using a soil water dependent root extraction function. Journal of Hydrology, 31 (1), 13–26.

Spokas K and Bogner J. Limits and dynamics of methane oxidation in landfill cover soils (2011). Waste Management, 31(5), 823–32.

Thomas, H. R. and He, Y. (1995). Analysis of coupled heat, moisture and air transfer in a deformable unsaturated soil. Géotechnique, 45(4), 677-689.